A. Charki
e-mail: Abderafi.charki@istia.univ-angers.fr

K. Diop

LASQUO,
Institut des Sciences et Techniques de
L'ingénieur d'Angers,
62 Avenue Notre Dame du Lac,
Angers 49000, France

S. Champmartin

A. Ambari

LAMPA,
Centre Arts et Métiers Paris Tech d'Angers,
2 Boulevard du Ronceray,
Angers Cedex 49035, France

Reliability of a Hydrostatic Bearing

This paper presents a methodology for evaluating the failure probability of fluid bearings, which are sensitive components for the design of machine rotors, mechatronic systems, and high precision metrology. The static and dynamic behavior of a fluid bearing depends on several parameters, such as external load, bearing dimensions, supply pressure, quality of the machined surfaces, fluid properties, etc. In this paper, the characteristics of a simple geometry hydrostatic bearing are calculated analytically in order to demonstrate the usefulness of the methodology and its pertinence to bearing design. Monte Carlo simulation and first order reliability method (FORM) are used to evaluate the probability of failure.

Keywords: hydrostatic bearing, fluid, reliability, Monte Carlo, FORM

1 Introduction

Fluid bearings are vital components of machines used in mechanical engineering, where their purpose is to feed and guide the rotation of transmission shafts. They are found in rotating machinery such as compressors and turbines. Their main advantage resides in superior stiffness and stability compared with alternative bearing technology. For feeding rotors, hydrodynamic bearings (where the pressure gradient is generated simply by the relative movement of the rotor) do not provide adequate boundary lubrication during shutdown and start-up phases. To enable rotating machinery to handle large loads when rotor rotation speed is zero and guarantee a relative eccentricity close to zero, hybrid bearings are used (an external source, e.g., an orifice, generates additional pressure gradient) [1–4].

However, if these are not very carefully designed and optimized, their dynamic behavior can be unstable and at worst cause a catastrophic breakdown of a machine. It is, therefore, important when studying their reliability to take into account both static and dynamic characteristics (which depend on several parameters, such as bearing length and diameter, number of feed orifices and their diameters, rotation speed, etc.) [2–4].

A new methodology for reliable bearing design that takes the different influential factors into account is herein proposed. This paper examines the static characteristics of a hydrostatic bearing in order to apply the methodology proposed for evaluating the failure probability of a bearing.

2 Reliability of a Fluid Bearing

2.1 Principle of Reliability. Reliability is a characteristic of a device expressed as the probability that it will accomplish a particular function under given conditions during a given time interval [5,6]. It can be deduced by estimating failure probability P_f.

Given the complexity of the failure domain and of the probability density function, which can bring into play a large number of variables, it is not easy to calculate the integral P_f, which is written as follows:

$$P_f = \int_{G(X_i)\le 0} f_{X_1,X_2,\ldots,X_n}(x_1,x_2,\ldots,x_n)dx_1dx_2,\ldots,dx_n = \text{Prob}\{(G(X_i)) \le 0\} \quad (1)$$

where $G(X_i)$ is the performance function. When $G(X_i) \le 0$, one is in the domain of a space-variant failure probability with random variables.

Aside from numerical integration methods, there exists a comprehensive theorem on evaluation of this probability integral. This theorem includes:

- An isoprobabilistic transformation of basic variables in a standard space where they become independent reduced centered Gaussian components.
- The search in the standard space for a surface limit state design point P^*, where the probability density is maximal. The failure probability is evaluated in the standard space using approximation methods.

Figure 1 shows the transformation of physical space into normalized space. H is the equivalent of G in the normalized space.

Failure probability is calculated analytically following transformation of physical space into normalized space with independent variables and determination of the failure point with the highest probability density—designated most probable failure point P^*, see Fig. 1.

The Monte Carlo method can, therefore, be applied but requires a long calculation time. Alternative methods based on approximation of the limit state function can be applied, such as the FORM and second order reliability method (SORM), for instance.

A comparison of different approximation methods has been drawn up by Madsen et al. [5] and Melchers [6]. These methods may be direct, make use of an optimization algorithm (the Rackwitz–Fiessler algorithm, for example), or use response surface method [3]. But above all, it is essential to define the performance function of the bearing being studied.

2.2 The Monte Carlo Method. Simulation methods make it possible to estimate the failure probability even when faced with complex laws of probability and nonlinear correlations between variables or limit state functions. However, the calculation times required by these methods may be prohibitive. The principle of Monte Carlo simulations is to apply the law of probability to repeated samples conjointly with the random vector and count the number of times the system produces a result in the failure

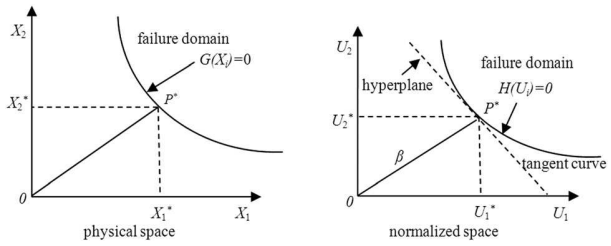

Fig. 1 Transformation of physical space into normalized space

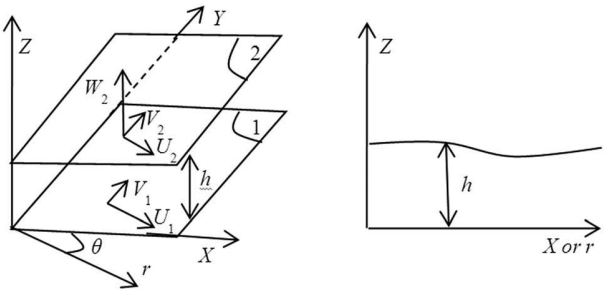

Fig. 2 Systems of axes and notation

domain. The failure probability may be expressed by the following relation:

$$P_f \approx \frac{1}{N}\sum_{i=1}^{N} I[G(X_i) \le 0] \tag{2}$$

where X_i is the vector of random variables, and the indicator function I is equal to 1 if the condition $G(X_i) \le 0$ is true and 0 if not. The evaluation of failure probability is accurate if the number of samples is sufficiently high.

One of the major drawbacks of the Monte Carlo method is the high number of simulations required in certain cases. Indeed, for a low failure probability, an inadequate number of simulations could lead to a significant degree of error.

2.3 FORM Method. The FORM method consists of estimating the reliability index β [6,7]. This method approximates the failure domain with a half-space delimited by a surface tangent hyperplane at design point P^*, as shown in Fig. 1. Thanks to the rotational symmetry of the normalized multinormal distribution, the failure probability can be easily approximated by

$$P_f = \Phi(-\beta) \tag{3}$$

where Φ is the standard normal distribution.

Design point P^* is determined by finding the limit state point closest to the origin of the normalized space. The design point is the solution of the following optimization problem:

$$\begin{cases} \beta = \text{distance} = \min\|U\| \\ H(U) = 0 \end{cases} \tag{4}$$

where H is the equivalent of G in the normalized space (see Fig. 1). U is the vector of random variables in the normalized space.

This constrained minimization problem is resolved using the Rackwitz–Fiessler algorithm and the design point is evaluated as

$$U^* = -\beta\alpha \tag{5}$$

The standardized gradient α of the limit state function, evaluated at design point $\boldsymbol{U}^*$, is determined by

$$\alpha = \frac{\nabla H(U^*)}{\|\nabla H(U^*)\|} \tag{6}$$

The reliability index β is then determined by

$$\beta = \frac{H(U^*) - \nabla H(U^*)\cdot\{U^*\}}{\|\nabla H(U^*)\|} \tag{7}$$

The tangent hyperplane equation (cf. Fig. 1) at design point U^* is

$$\breve{H}(U) = \beta + \sum_{i=1}^{n} \alpha_i u_i \tag{8}$$

This method gives an accurate result when the limit state is linear in the standard space. It becomes inaccurate when the performance function is highly nonlinear around the design point or when there are significant secondary minima.

2.4 Definition of the Performance Function of a Fluid Bearing. The performance function of a fluid bearing depends on the choice of different parameters, such as radius, the number of orifices, film thickness, feed pressure, etc.

The failure probability of a fluid bearing is determined via the following performance function; this is defined as the difference between the load carrying capacity corresponding to an operating thickness h and the maximum load capacity corresponding to a critical level h_c.

$$G(X) = W_e(X) - W_c(X) \tag{9}$$

where X is the vector of random variables, W_c is the maximum load capacity of the bearing, and W_e is the operating load capacity. The values for these two load capacities depend on the bearing parameters and are estimated by using the equations presented in the next section. Failure of a bearing occurs when the film thickness falls below critical thickness h_c.

3 Modeling of a Hydrostatic Bearing

3.1 Reynolds Equation. Detailed explanations of how the simplifying assumptions were established for this study are given by Gross et al. [1]:

- The flow is continuous.
- The fluid is Newtonian.
- The flow is laminar and isothermal.
- The external mass forces and inertia force are negligible.
- There is no slippage between the fluid and the contact surfaces.
- The curvature of the fluid is ignored.
- The measured thickness of the fluid film is always small compared with the other dimensions of the contact area (indeed this is the underlying assumption of lubrication theory).
- The velocity of one surface (surface 1) is tangent to that surface at all points (cf. Fig. 2), and given that specific gravity and viscosity do not vary with film thickness, the origin of the axes system is located at one of the contact surfaces.

Figure 2 is a representation of the thin fluid film region. The projection is such that the z coordinate corresponds to film thickness. The velocity of a point on surface 1 is given by the U_1, V_1, W_1 components and is related to the r, θ, and z coordinates. In the same way, the velocity of a point on surface 2 is given by the U_2, V_2,W_2 components.

Using the primitive equations for thin viscous films, it is possible, with due regard for the geometric and kinematic conditions, to determine the thin film flow parameters and in particular load-bearing capacity, flow-rate, and stiffness.

These equations can be deduced from the equations for continuous media mechanics applied to a Newtonian fluid [8–10].

Using the simplifying assumptions already cited, the conservation equations for the mass and momentum can be written thus

$$\frac{1}{r}\frac{\partial}{\partial r}(ru)+\frac{1}{r}\frac{\partial v}{\partial \theta}+\frac{\partial w}{\partial z}=0 \tag{10}$$

$$\frac{\partial u}{\partial t}+u\frac{\partial u}{\partial r}+\frac{v}{r}\frac{\partial u}{\partial \theta}+w\frac{\partial u}{\partial z}-\frac{v^2}{r}=-\frac{1}{\rho}\frac{\partial P}{\partial r}+\upsilon\left[\frac{1}{r}\frac{\partial}{\partial r}\left(r\frac{\partial u}{\partial r}\right)-\frac{u}{r^2}+\frac{1}{r^2}\frac{\partial^2 u}{\partial \theta^2}+\frac{\partial^2 u}{\partial z^2}-\frac{2}{r^2}\frac{\partial v}{\partial \theta}\right] \tag{11}$$

$$\frac{\partial v}{\partial t}+u\frac{\partial v}{\partial r}+\frac{v}{r}\frac{\partial v}{\partial \theta}+w\frac{\partial v}{\partial z}-\frac{uv}{r}=-\frac{1}{\rho r}\frac{\partial P}{\partial \theta}+\upsilon\left[\frac{1}{r}\frac{\partial}{\partial r}\left(r\frac{\partial v}{\partial r}\right)-\frac{v}{r^2}+\frac{1}{r^2}\frac{\partial v}{\partial \theta}+\frac{\partial^2 u}{\partial z^2}-\frac{2}{r^2}\frac{\partial u}{\partial \theta}\right] \tag{12}$$

$$\frac{\partial w}{\partial t}+u\frac{\partial w}{\partial r}+\frac{v}{r}\frac{\partial w}{\partial \theta}+w\frac{\partial w}{\partial z}=-\frac{1}{\rho}\frac{\partial P}{\partial z}+\upsilon\left[\frac{1}{r}\frac{\partial}{\partial r}\left(r\frac{\partial w}{\partial r}\right)+\frac{1}{r^2}\frac{\partial^2 w}{\partial \theta^2}+\frac{\partial^2 w}{\partial z^2}\right] \tag{13}$$

Using the assumptions inherent to lubrication theory, the expressions for the fluid velocity components can be obtained relative to r and θ and in relation to the pressure gradient components and the velocity components at the surface.

$$u=\frac{1}{2\mu}\frac{\partial P}{\partial r}Z(Z-h)+\frac{h-z}{h}U_1+\frac{z}{h}U_2 \tag{14}$$

$$v=\frac{1}{2\mu r}\frac{\partial P}{\partial \theta}z(z-h)+\frac{h-z}{h}V_1+\frac{z}{h}V_2 \tag{15}$$

Integration along the velocity components axis (Oz) of the conservation of momentum equation gives the following Reynolds equation [1]:

$$\frac{\partial}{\partial r}\left(\frac{\rho r h^3}{\mu}\frac{\partial P}{\partial r}\right)+\frac{\partial}{\partial \theta}\left(\frac{\rho h^3}{\mu r}\frac{\partial P}{\partial \theta}\right)=6r\rho(U_1-U_2)\frac{\partial h}{\partial r}+6\rho(V_1-V_2)\frac{\partial h}{\partial \theta}+6rh\frac{\partial}{\partial r}[\rho(U_1+U_2)]+6h\frac{\partial}{\partial \theta}[\rho(V_1+V_2)]+6\rho h(U_1+U_2)+12\rho r W_2+12rh\frac{\partial \rho}{\partial t} \tag{16}$$

3.2 Practical Application to a Hydrostatic Bearing. In order to demonstrate our methodology, we propose here to examine a simple example by applying Reynolds equation to a groove hydrostatic bearing with feed orifices as shown in Fig. 3.

In this analytical study, the bearing is assumed to be symmetrical relatively to angle θ, and the feed pressure P_0 is constant at radius R_0.

In the static case, the simplified Reynolds equation thus becomes

$$\frac{\partial}{\partial r}\left[\frac{\rho r h^3}{\mu}\frac{\partial P}{\partial r}\right]=0 \tag{17}$$

The pressure limit conditions are

$$\begin{aligned} r\le R_1;&\quad P=P_a\\ r=R_0;&\quad P=P_0\\ R_1\le r\le R_0;&\quad P=P_{r1}\\ R_0\le r\le R_2;&\quad P=P_{r2}\\ r=R_2;&\quad P=P_a \end{aligned}$$

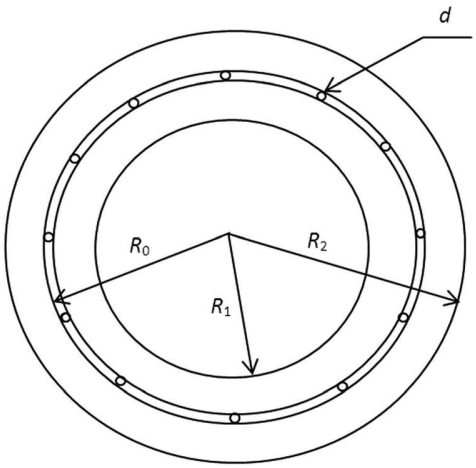

Fig. 3 Configuration of the bearing studied

Integration of Eq. (17) with limit conditions gives the pressure expressions

$$P_{r1}=\frac{1}{\ln\frac{R_0}{R_1}}\left[P_0\ln\frac{r}{R_1}-P_a\ln\frac{r}{R_0}\right] \tag{18}$$

$$P_{r2}=\frac{1}{\ln\frac{R_0}{R_2}}\left[P_0\ln\frac{r}{R_2}-P_a\ln\frac{r}{R_0}\right] \tag{19}$$

3.3 Performance Function of a Hydrostatic Bearing. Integration of surface pressure gives the load-bearing capacity expression

$$W=\pi\left(R_2^2-R_1^2\right)P_a+\frac{\pi}{2}(P_0-P_a)\left(\frac{R_1^2-R_0^2}{\ln\frac{R_0}{R_1}}-\frac{R_2^2-R_0^2}{\ln\frac{R_0}{R_2}}\right) \tag{20}$$

This load-bearing capacity value may be determined relatively to fluid film thickness h. For this, simply replace pressure P_0 values with values obtained for different fluid film thicknesses h due to sustained volume flow rate.

Integration of radial velocity at the rotor and stator transverse surface gives the expression for flow-rate through the bearing, and is written as follows:

$$Q_S=\frac{\pi h^3}{6\mu}(P_0-P_a)\left(\frac{1}{\ln\frac{R_1}{R_0}}+\frac{1}{\ln\frac{R_2}{R_0}}\right) \tag{21}$$

The input flow into the orifices is written thus

$$Q_0=nC_d\frac{\pi d^2}{4}\sqrt{\frac{2(P_S-P_0)}{\rho}} \tag{22}$$

where n is the number of orifices, C_d is the discharge coefficient, d is the orifice diameter (m), and P_s is the source pressure (Pa).

The specific orifice supply pressure P_0 is obtained by equalizing the input volume flow rate Q_o and the output volume flow rate Q_s.

Table 1 Hydrostatic bearing parameter values

Designation	Value
R_1 (mm)	30
R_0 (mm)	48
R_2 (mm)	75
ρ (kg/m^3)	794.7
P_a (Pa)	10^5
P_s (Pa)	7×10^5
d (mm)	0.15
C_d	0.7
μ (Pa·s)	0.0012
n (number of orifices)	12

Table 2 Hydrostatic bearing random variables

Variables	Mean	CV	Distribution
R_1 (mm)	30	2%	normal
R_0 (mm)	48	2%	normal
R_2 (mm)	75	2%	normal
d (mm)	0.15	2%	normal

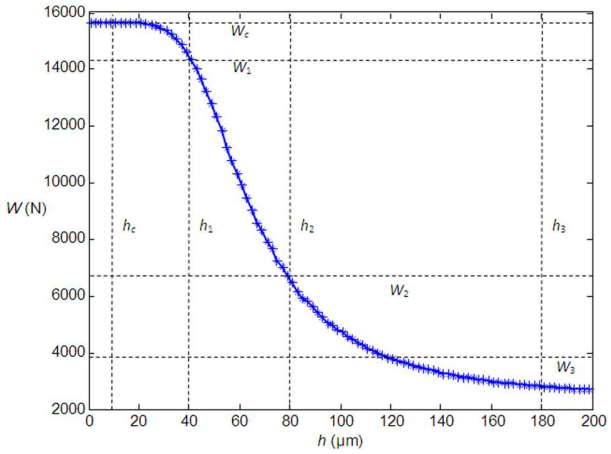

Fig. 4 Load carrying capacity versus film thickness

The performance function G for evaluating the failure probability is deduced from the relations in Eqs. (9) and (20) and is expressed thus,

$$G(X) = \frac{\pi\left(P_0^h - P_0^{h_c}\right)}{2}\left[\frac{R_1^2 - R_0^2}{\ln\dfrac{R_0}{R_1}} - \frac{R_2^2 - R_0^2}{\ln\dfrac{R_0}{R_2}}\right] \tag{23}$$

where P_0^h and $P_0^{h_c}$ are, respectively, the pressure P_0 calculated for the fluid film thickness h and h_c using the expressions in Eqs. (21) and (22). The performance function G can be evaluated by using the vector of random variables $X = \{\mu, \rho, C_d, d, P_S, R_1, R_2, R_0\}$.

4 Application

Let us now consider the hydrostatic bearing described in Sec. 3.2. The hydrostatic bearing parameters used for calculations are shown in Table 1. Table 2 shows the variables used for estimating failure probability. This table gives the mean, the coefficient of variation (CV), and the associated distribution law for each variable.

Table 3 Failure probability with FORM and Monte Carlo

Method	Probability P_f	Time (s)
FORM ($h_{e1} = 40\,\mu$m)	0.1183	30.12
FORM ($h_{e2} = 80\,\mu$m)	0.0245	32.33
FORM ($h_{e3} = 180\,\mu$m)	0.0028	33.37
Monte Carlo ($h_{e1} = 40\,\mu$m)	0.1195	212.37
Monte Carlo ($h_{e2} = 80\,\mu$m)	0.0299	792.33
Monte Carlo ($h_{e3} = 180\,\mu$m)	0.0030	9.6978 E + 03

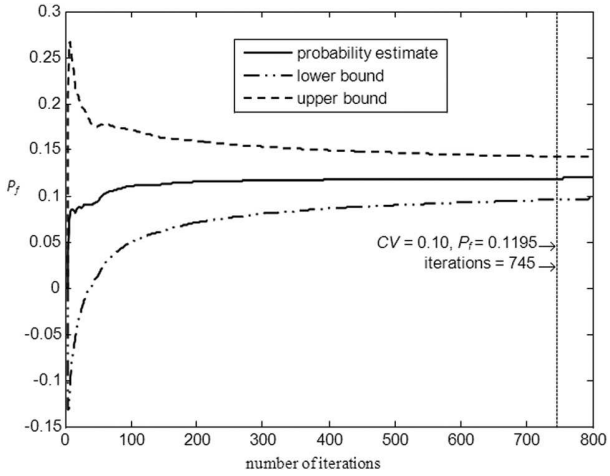

Fig. 5 Failure probability obtained by Monte Carlo for $h_{e1} = 40\,\mu$m

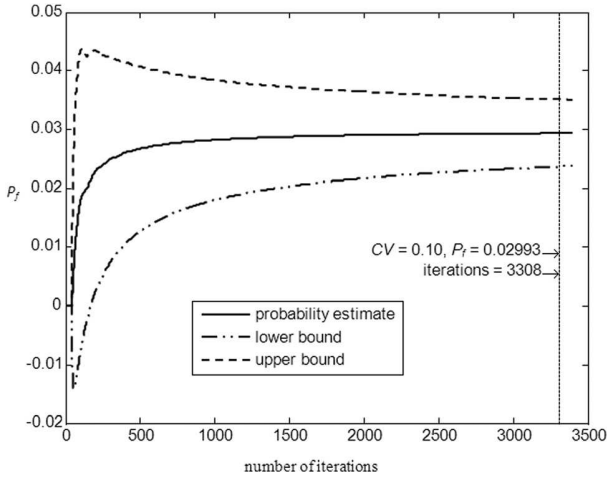

Fig. 6 Failure probability obtained by Monte Carlo for $h_{e2} = 80\,\mu$m

Figure 4 shows changes in load-bearing capacity W relative to fluid film h obtained from Eq. (20).

For the evaluation of failure probability of the bearing studied, we assume that $h_c = 10\,\mu$m, and we consider three operating load capacities $W_{e1} = 1.4512\,\text{E} + 04\,\text{N}$, $W_{e2} = 6.5870\,\text{E} + 03\,\text{N}$, and $W_{e3} = 2.8235\,\text{E} + 03\,\text{N}$, corresponding to, respectively, three film thickness $h_{e1} = 40\,\mu$m, $h_{e2} = 80\,\mu$m, and $h_{e3} = 180\,\mu$m. The maximum load capacity $W_c = 1.5663\,\text{E} + 04\,\text{N}$ is obtained for h_c.

Table 3 shows the results obtained with the Monte Carlo and FORM methods for three operating load carrying capacities W_{e1}, W_{e2}, and W_{e3} is corresponding to three respective operating

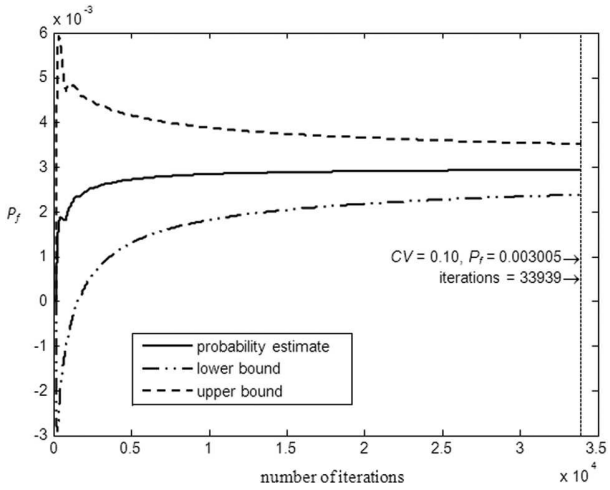

Fig. 7 Failure probability obtained by Monte Carlo for $h_{e3} = 180\,\mu$m

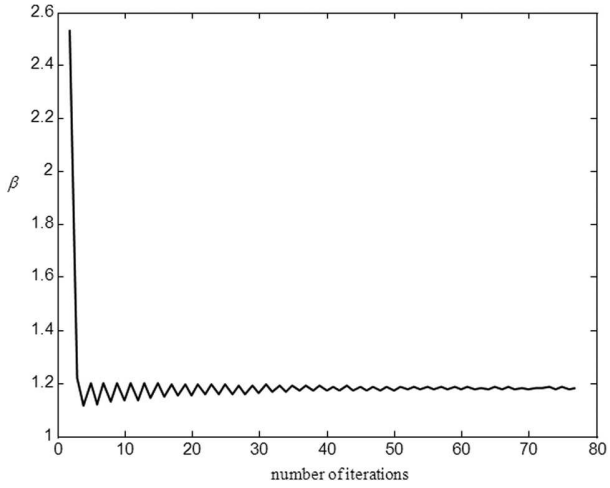

Fig. 8 Index reliability obtained by FORM for $h_{e1} = 40\,\mu$m

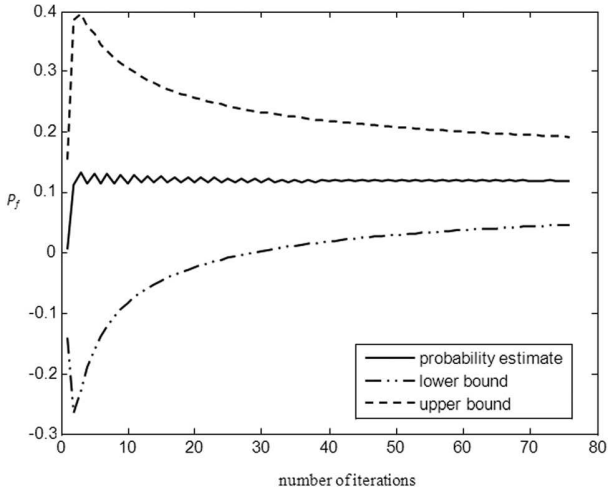

Fig. 9 Failure probability obtained by FORM for $h_{e1} = 40\,\mu$m

thicknesses h_{e1}, h_{e2}, and h_{e3}. The estimation of P_f for the three operating load capacities $W_{e1} = 1.4512\,\text{E} + 04\,\text{N}$, $W_{e2} = 6.5870\,\text{E} + 03\,\text{N}$, and $W_{e3} = 2.8235\,\text{E} + 03\,\text{N}$ is calculated with $W_c = 1.5663\,\text{E} + 04\,\text{N}$ using the performance function in Eq. (23).

The probability of failure diminishes as film thickness increases; it also diminishes as nominal load capacity deviates more from critical load capacity.

Figures 5, 6, and 7 give an estimation of failure probability P_f with the Monte Carlo method for $h_{e1} = 40\,\mu$m, $h_{e2} = 80\,\mu$m, and $h_{e3} = 180\,\mu$m. The results of P_f are obtained with a confidence interval of 95%. As shown in Figs. 5, 6, and 7, the results converge giving a coefficient of variation of $CV = 0.1$ for the P_f values.

Figures 8 and 9 show, respectively, the convergence of index reliability and failure probability estimated with FORM for the film thickness $h_{e1} = 40\,\mu$m. Convergence is rapidly achieved regardless of the film thickness and the level of failure probability.

It is clear that the calculation is very long using the Monte Carlo method, especially for very low failure probabilities, as shown in Table 3. FORM remains a useful tool for the failure probability estimation of a bearing.

5 Conclusion

In this paper, we present a new methodology that is of practical use in bearing design.

The approach developed here demonstrates the value of estimating failure probability and shows how bearing design may be optimized via reliability criteria. A simple application is used to illustrate the argument, that of a hydrostatic bearing fed with a pressure source via orifices.

To calculate the failure probability of the bearing, two operating load capacities are examined, one of which is close to the critical load capacity associated with the minimum thickness below which the bearing cannot function while the other is nowhere near the critical load capacity. Failure probability increases as the fluid film value decreases.

The results obtained using the FORM and Monte Carlo methods suggest that the methodology developed here is worth exploring with other configurations, for instance, with a larger number of variables. FORM, as is explained in the literature, is advantageous from the point of view of calculation times. The nonlinear limit function of G can also be approximated using SORM, and the error of approximation can also be analyzed for all proposal methods in this article.

The methodology expounded here is applied in the LASQUO and LAMPA laboratories for other types of bearings (cylindrical, etc.).

Nomenclature

P_0 = specific orifice supply pressure (Pa)
P_a = atmospheric pressure (Pa)
R_1 = inner radius (m)
R_0 = orifice crown radius (m)
R_2 = outer radius (m)
r = elementary radius (m)
ρ = fluid specific gravity (kg/m^3)
μ = dynamic viscosity (Pa·s)
h = fluid film thickness between the upper and lower sides (m)

References

[1] Gross, W. A., Matsch, L. A., Castelli, V., Eshel, A., Vohr, J. H., and Wildmann, M., 2008, *Fluid Film Lubrication*, Wiley, New York.
[2] Charki, A., Bigaud, D., and Guerin, F., 2013, "Behavior Analysis of Machines and System Air, Hemispherical Spindles Using Finite Element Modeling," Ind. Lubr. Tribol., **65**(4), pp. 272–283.
[3] Charki, A., Elsayed, E. A., Guerin, F., and Bigaud, D., 2009, "Fluid Thrust Bearing Reliability Analysis Using Finite Element Modeling and Response Surface Respond," Int. J. Qual. Eng. Technol., **1**, pp. 188–205.

[4] Charki, A., Diop, K., Champmartin, S., and Ambari, A., 2013, "Numerical Simulation and Experimental Study of Thrust Air Bearings With Multiple Orifices," Int. J. Mech. Sci., **72**, pp. 28–38.
[5] Madsen, H. O., Krenk, S., and Lind, N. C., 1986, *Structural Method of Safety*, Prentice-Hall, Englewood Cliffs, NJ.
[6] Melchers, R. E., 1999, *Structural Reliability Analysis and Prediction*, 2nd ed., Wiley, New York.
[7] Di Sciuva, M., and Lomario, D., 2003, "A Comparison Between Monte Carlo and FORMs in Calculating the Reliability of a Composite Structure," Compos. Struct., **59**, pp. 155–162.
[8] De Pellegrin, D. V., and Hargreaves, D. J., 2012, "An Isoviscous, Isothermal Model Investigating the Influence of Hydrostatic Recesses on a Spring-Supported Tilting Pad Thrust Bearing," Tribol. Int., **51**, pp. 25–35.
[9] Jang, G. H., and Kim, Y. J., 1999, "Calculation of Dynamic Coefficients in a Hydrodynamic Bearing Considering Five Degrees of Freedom for a General Rotor-Bearing System," ASME J. Tribol., **121**(3), pp. 499–505.
[10] Srikanth, D. V., Chaturvedi, K. K., and Reddy, A. C. K., 2012, "Determination of a Large Tilting Pad Thrust Bearing Angular Stiffness," Tribol. Int., **47**, pp. 69–76.